Uncovering new global risks from commercial chemicals in air

John Liggio (john.liggio@canada.ca)
Environment Canada https://orcid.org/0000-0003-3683-4595
Qifan Liu
Environment and Climate Change Canada
Li Li
University of Nevada Reno
Xianming Zhang
Environment and Climate Change Canada
Amandeep Saini
Environment and Climate Change Canada https://orcid.org/0000-0003-0880-1147
Wenlong Li
Environment and Climate Change Canada
Hayley Hung
Environment and Climate Change Canada
Chunyan Hao
Ontario Ministry of the Environment
Kun Li
Paul Scherrer Institute
patrick Lee
Environment Canada
Jeremy Wentzell
Environment and Climate Change Canada
Chunyan Huo
Environment and Climate Change Canada
Shao-Meng Li
Peking University
Tom Harner
Environment and Climate Change Canada

Physical Sciences - Article

Keywords: commercial chemicals, air pollution, harmful chemicals

Posted Date: March 12th, 2021

DOI: https://doi.org/10.21203/rs.3.rs-209026/v1

Version of Record: A version of this preprint was published at Nature on December 15th, 2021. See the published version at https://doi.org/10.1038/s41586-021-04134-6.

Abstract

Commercial chemicals are used extensively across global urban centers, posing a potential exposure risk to 4.2 billion people, which accounts for 55% of the global population. Harmful chemicals are often assessed and regulated based on their environmental persistence, bioaccumulation, and toxic properties, under international and national initiatives such as the Stockholm Convention. However, current regulatory frameworks largely rely upon knowledge of the properties of the parent chemicals, with minimal consideration given to their atmospheric transformation products. This is mainly due to a significant lack of experimental data, as identifying transformation products in complex mixtures of airborne chemicals is an immense analytical challenge,hence making a comprehensive and reliable risk assessment for harmful chemicals currently unachievable. Here, we develop a novel framework, combining laboratory and field experiments, non-target analysis techniques, and in-silico modelling, to identify and assess the hazards of airborne chemicals, which takes into account atmospheric chemical reactions. By applying this framework to organophosphate flame retardants, as representative chemicals of emerging concern, we find that their transformation products are globally distributed across 18 megacities, representing a previously unrecognized exposure risk for the world's urban populations. Furthermore, the transformation products can be up to an order of magnitude more persistent, environmentally mobile, and toxic than the parent chemicals. The results indicate that the overall human and environmental risks associated with flame retardants could be significantly underestimated, while highlighting a strong need to include atmospheric transformations in the development of regulations for all harmful chemicals moving forward.

Main Text

In response to the environmental and health risks posed by commercial chemicals, substantial efforts have been made to prioritize and regulate chemicals of emerging concern (CECs).[9] These efforts usually occur in the context of international[6] and national regulatory initiatives such as the US Toxic Substances Control Act,[10] and the European Union's Registration, Evaluation, Authorization and Restriction of Chemicals program.[11] Most regulatory measures begin with an assessment of a chemical's potential for causing adverse effects in organisms and the environment, mainly via their ability to resist abiotic or biotic degradation (Persistence; **P**), accumulate in the tissues of organisms or humans (Bioaccumulation; **B**), and exert adverse health outcomes (Toxicity; **T**) (i.e., **PBT**). However, the current PBT assessment approach for CECs is primarily based upon available physicochemical and toxicological data for parent chemicals, with minimal consideration given to the products associated with their atmospheric transformations.

During their residence time in the atmosphere, CECs will be transformed into other species through photooxidation.[12] Consequently, humans and ecosystems are exposed to both the parent CECs and a diverse suite of transformation products. However, CEC transformation products formed in air are not measured in current international and national atmospheric monitoring networks despite their intent of tracking global and regional distributions of CECs.[13-15] As a result, only a fraction of the CEC-related chemicals which exist have been monitored. This is of particular concern should the unknown transformation products be more hazardous than their precursor species, thus making an accurate risk assessment of CECs unattainable.

The lack of transformation product identification and information associated with their PBT is in part, due to the current target-analysis approach to identifying harmful airborne CECs.[13,14] It is also a result of the immense analytical challenge associated with tracking complex mixtures of airborne chemicals.[7] In particular, atmospheric transformation products, for which no analytical standards exist, are very difficult to distinguish from other species present in complex mixtures. With recent developments in high-resolution mass spectrometry, limited studies have attempted to utilize non-target analysis (NTA) techniques to identify unknown pollutants within complex mixtures without specifically targeting individual parent molecules.[16,17] Although NTA techniques can help to infer chemical formulae for unknown pollutants, they cannot provide the exact chemical structures of these pollutants, or determine the mechanistic pathways through which they are formed and hence their chemical origin.[18] Such missing information hinders a comprehensive risk assessment of CECs that serves as the scientific basis for regulations.

Organophosphate flame retardants (OPFRs) are a group of CECs that has garnered significant international attention.[8] They are widely used in consumer and industrial products to reduce the risk of fire, and have been mass-produced due to the regulation of traditionally used polybrominated diphenyl ether (PBDE) flame retardants in recent years.[19] While OPFRs represent a type of CEC in the early stages of risk assessment, there is serious concern that they may be regrettable alternatives to PBDEs,[19] as suggested by their ubiquity in the global atmosphere,[2] long-range transport potential,[20] and demonstrated toxicity.[8] However, like many other CECs, the atmospheric chemistryhas not been considered in their overall risk assessment, despite the certainty of atmospheric chemical reactions.[12] This underscores the need for new approaches for conducting CEC risk assessment, rooted in a framework that takes into account the formation of transformation products, their presence in the ambient air, and their associated PBT properties. Below we describe the development and application of such a novel framework that considers the atmospheric chemistry of CECs.

Hazard assessment framework

The framework consists of three components: laboratory oxidation experiments, a non-target analysis, and an in-silico hazard assessment (Fig. 1). The first step is to simulate atmospheric photooxidation of CECs using an oxidation flow reactor,[21] combined with online transformation product detection.[22] The laboratory oxidation experiments provide comprehensive information on the atmospheric photooxidation of CECs, including the rate of photooxidation reactions (i.e., reaction kinetics), how the parent chemicals form products (i.e., atmospheric transformation mechanisms), and what products are formed (i.e., a product list). Consequently, this step forms the basis of molecular identification of transformation products in field samples, as discussed below.

Non-target analysis is then applied to both laboratory samples (derived from photooxidation experiments) and field samples (ambient air samples). NTA of field samples often yields extremely complex mass spectra as a result of thousands of unknown species.[17] However, through the application of NTA to laboratory samples (step a in Fig. 1), we can reduce this complexity by obtaining fingerprint-like features associated with transformation products (e.g., retention times, elemental formulae, chemical structures, and isotopic patterns; see Methods) arising from any given CEC. These fingerprint-like features serve as “chemical standards”, which can be used to guide the analysis of transformation products in complex field samples. This approach enables unambiguous identification of transformation products in field samples, and the ability to determine the parent chemicals from which they originated (an essential requirement for future chemical regulations).

Finally, fed with the molecular structures of the transformation products identified in laboratory oxidation experiments, well-established in-silico models are used to predict their behavior and fate, and thus assess their PBT in a holistic multimedia environment (step b in Fig. 1). As an advantage to in-vitro and in-vivo experiments, an in-silico assessment can assess thousands of chemicals in a high-throughput, cost-effective manner. Notably, the PBT hazards are quantified as numerical values reflecting a transformation product’s impacts across multiple environmental media and multiple organs, which facilitates screening and prioritization for decision-making, and risk communication.

The new framework bridges the knowledge gap between chemical formulae (typically obtained via NTA) and chemical structures of CEC transformation products. This is particularly important given that chemical structures form the basis of the environmental and human health risk assessment of CECs,[23] and since chemical identification in current NTA approaches can be ambiguous (one empirical formula can correspond to multiple chemical structures).[18] Furthermore, the framework provides a new avenue for including transformation products in routine national and international monitoring programs and prioritizing transformation products of high concern for further scrutiny (step c and d in Fig. 1). In summary, the framework presents an experimentally confirmed, structure-based strategy for assessing potential hazardous outcomes associated with atmospherically transformed CECs, which has not been considered previously.

Application to organophosphate flame retardants

In this illustrative case, our framework was applied to 9 OPFRs (Extended Data Fig. 1) which represented the most frequently detected OPFRs in ambient air.[13] Upon photooxidation in laboratory experiments, 186 transformation products were detected, representing early (formed through less than three reaction steps) to later generation transformation products (Supplementary Table 1). Knowledge of the product formulae and principles of organic reactions were used to infer the most likely transformation mechanisms and to elucidate the molecular structures of transformation products. Based upon individual mechanisms (Supplementary Figs. 1 and 2), a general reaction scheme that includes three main channels can be formulated for OPFRs (Extended Data Fig. 2).

Use of NTA on the laboratory samples derived from 5 reacted OPFRs (the five most abundant OPFRs in the ambient air)[13] resulted in chromatographic and mass spectral information for 27 products (Supplementary Table 2). This information was then used to screen NTA data from field samples collected in 18 megacities under the Global Atmospheric Passive Sampling-Megacities program (see Methods). In the field samples, 20 transformation products (derived from 5 OPFRs) were characterized. Of these transformation products, 11 can be assigned to known molecular structures (i.e., identified products; Extended Data Figs. 3 and 4) and 9 were derived from chlorinated OPFRs but without known structures (i.e., unidentified products; Supplementary Table 3). The 11 identified products, with detection frequencies of 94–100% (Supplementary Table 4), can be further divided into two groups based upon their structures: 7 chlorinated products (identified based upon their retention times, mass peaks, and isotopic patterns) and 4 non-chlorinated products. These transformation products are primarily early-generation products, consistent with the expectation of short oxidation timescales associated with urban regions.[24] These 20 compounds are the first reported measurements of airborne OPFR transformation products. However, we expect that they represent the tip of the iceberg, as more transformation products are likely to be found in the atmosphere, e.g., in rural and remote regions where more highly aged air masses favor the formation of additional products.[25]

The global distribution of the 11 identified OPFR transformation products is shown in Fig. 2, using volume normalized signal intensity (counts m^{-3}) as a proxy for air concentration (in the absence of authentic standards). The geographic distribution in Fig. 2 reflects the ubiquity of transformation products in the global atmosphere arising from the widespread use of OPFRs. Also, high levels of parent OPFRs in a given city result in correspondingly high levels of transformation products (Fig. 3a). For example, the total normalized signal intensities of 11 identified products are highest in London, UK, and New York, USA (2–35 times higher than other cities), consistent with the highest concentrations of parent OPFRs (sum=14,000 pg m^{-3}).[13] Further analysis also indicates that there is a seasonality associated with transformation product formation. For example, among the urban samples from Toronto, Canada,[26] the ratio of product to parent OPFR signal intensity (R_{signal}; a parameter that reflects the extent of photooxidation) is up to 6 times higher in summer than in winter (Fig. 3b). Given that the increased light levels in summer favor atmospheric photooxidation, this observed seasonal contrast verifies that the identified species are a result of photochemical reactions.

The ubiquity of OPFR transformation products (Fig. 2) is especially concerning given their in-silico derived PBT properties illustrated in Fig. 4. Fig. 4a shows the fold changes in the PBT of 186 transformation products relative to the 9 investigated parent OPFRs; a fold change higher than 1 indicates an increased environmental concern associated with a product relative to its precursor. Fig. 4a indicates that the overall persistence, i.e., the overall ability to resist various degradation processes across all environmental media, for the transformation products of chlorinated OPFRs are on average 2.5 times higher than their originating parent molecules (90% of the red data points in Fig. 4a lie to the left of the dashed line; for chemical-specific results, see Extended Data Fig. 5). Conversely, transformation products of non-chlorinated OPFRs (blue data points in Fig. 4a) are on average 25% less persistent. This contrasting observation arises from differences in the multimedia mass distributions (atmosphere vs. surface media including surface water, soil, and sediment) of the transformation products derived from chlorinated and non-chlorinated OPFRs. Specifically, transformation products of chlorinated OPFRs, have a higher affinity for surface media due to an increase in octanol-air partition coefficients (K_{OA}) from atmospheric photooxidation (Extended Data Fig. 6). Since almost all the product species investigated here have an order-of-magnitude slower rate of degradation in surface media than the rate of atmospheric photooxidation (Supplementary Fig. 3), such a preference for surface media preserves more of the total mass within the environment, resulting in a higher overall persistence. Conversely, atmospheric photooxidation of non-chlorinated OPFRs forms products with a higher fraction present in the atmosphere, leading to lower overall persistence. Nevertheless, 7 of the 9 OPFRs investigated form transformation products of which at least 5% (and up to 93%) are more persistent than the parents (Fig. 4b).

Transformation products of all OPFRs are orders of magnitude less bioaccumulative in aquatic biota than their corresponding parents (Fig. 4a and Extended Data Fig. 7). Atmospheric oxidation adds oxygen-containing functional groups to OPFRs and generates more hydrophilic transformation products, as demonstrated by their lower (relative to parent molecules) octanol-water partition coefficients (K_{OW}; see Extended Data Fig. 6). Hence, these products are more easily eliminated through gill respiration in aquatic animals and are thus associated with reduced bioaccumulation potential.[27] However, the increase in hydrophilicity does not always imply a reduced environmental concern, as a chemical will exhibit increased environmental mobility if its K_{OW} is lower than 10^4,[28] as is the case for 91% of the transformation products investigated here. This makes many of these products more accessible to aquatic biota and more difficult to remove from water through traditional water treatment procedures,[28] implying an additional risk to the health of aquatic ecosystems and to the safety of drinking water.

The systemic toxicity, i.e., the toxicity to the entire animal, differs greatly between parent OPFRs and transformation products (Fig. 4a). While some chlorinated OPFRs can form less toxic products, the majority of non-chlorinated OPFRs form products up to an order of magnitude more toxic than their corresponding parents (Fig. 4a). This is consistent with photooxidation, which can toxify non-chlorinated OPFRs through the addition of more toxicologically active functionality, such as carbonyl groups.[29] Conversely, photooxidation can also detoxify chlorinated OPFRs by substituting more toxicologically active structures (e.g., chlorine) with less active moieties such as hydroxyl groups. It should be noted that recent experimental evidence indicates certain transformation products may also cause adverse toxicological effects.[30] For example, product TCPP-21 and TDCPP-14 (8.0-fold and 3.7-fold increase in relative LD50 ratio respectively; Extended Data Fig. 8) have been confirmed to be able to disrupt endocrine receptors in animals.[30] Moreover, all the transformation products investigated here are predicted to form a significant fraction (24–89%) of more toxic transformation products (Fig. 4b). We also note that all but three of the transformation products identified in ambient megacity samples are more toxic than their parent compounds (Extended Data Fig. 8).

The current results have profound implications for the ongoing assessment of hazardous outcomes of CECs. The global atmospheric ubiquity of OPFR transformation products shown here, combined with their tendency to be more persistent, environmentally mobile, and toxic, than their parent chemicals indicates that the human and environmental risks of OPFRs in current assessments which focus on parent compounds alone, may be underestimated. Including atmospheric transformations in the assessment of OPFRs is hence a requirement for determining the actual hazard associated with their use as PBDE replacements. Furthermore, the new framework described herein is

transferable to any CEC, as the vast majority of commercial chemicals released to air will be subjected to atmospheric transformations. It also provides a holistic means to include atmospheric transformation products of CECs in future monitoring networks, exposome studies,[31] and chemical management practices.

Finally, it is widely recognized that $PM_{2.5}$ (particulate matter with a diameter of smaller than 2.5 micrometers) is a major global human health concern.[32] Since many CECs (including OPFRs) are components of $PM_{2.5}$, global efforts in reducing $PM_{2.5}$ levels might also be expected to reduce exposure to CECs and their transformation products. However, as shown in Extended Data Fig. 9, the global distribution of OPFR transformation products in air observed here is clearly skewed to high-income nations (and lowest in low-income nations).[33] Conversely, global $PM_{2.5}$ mass concentrations are highest in lower-middle-income nations and lowest in high-income nations. While there are clearly other factors contributing to this pattern, these opposing trends suggest that the impact of commercial chemicals and their transformation products in the atmosphere, will be independent of having successfully reduced $PM_{2.5}$ levels. It may also act as an early warning to both high and low-income nations, highlighting the need to tackle both $PM_{2.5}$ reductions and chemical exposures simultaneously.

Methods

Global Atmospheric Passive Sampling-Megacities (GAPS-MC)

Sampling details. The GAPS-MC network consists of 18 megacities across the globe with a population ranging from 2 million to 22 million.[13] A representative site for each megacity was chosen such that they were well away from potential sources of targeted CECs and persistent organic pollutants (POPs) and with an unobstructed air flow and preferably centrally located within the city. Sampling dates are shown in Extended Data Table 1. Further details regarding the coordinates and site characteristics have been described previously.[13]

Polyurethane foam disk passive air samplers (PUF-PAS; Tisch Environmental, 14 cm diameter, 1.35 cm thickness, 370 cm^2 surface area) were used for sampling during the GAPS-MC project in 2018–2019. This double-dome configuration of PAS has been previously used for GAPS network sampling of a range of gas- and particle-phase CECs and POPs.[2,13] Pre-cleaning of PUF disks was performed via pressurized liquid extraction with an accelerated solvent extractor (ASE) instrument (ASE 350, Dionex Corporation, Sunnyvale, CA, USA) using acetone, petroleum ether and acetonitrile solvents. The cleaned PUFs for deployment were stored in pre-cleaned amber glass jars (1L). All the pre-deployment cleaning of sampling media was performed in the laboratories of Environment and Climate Change Canada, Toronto and shipped to international collaborators. PUF-PAS were deployed for 2–3 months at each site. GAPS-MC samples were collected from different megacities across different seasons. To further investigate the seasonal variations of OPFR transformation products, PUF-PAS from another sampling campaign were used.[26] These samples were deployed in downtown, Toronto, Canada (same location as of GAPS-MC site), from August 16 to September 16, 2016 (representing summertime) and from December 16, 2016 to January 17, 2017 (representing wintertime).

Extraction procedure. PUF-PAS samples were extracted using an ASE instrument with the combination of petroleum ether and acetone solvents (5:1, v/v for PUF-PAS samples; 3:1, v/v for flow reactor samples). The PUF-PAS extracts were then reduced to 0.5 mL using rotary evaporation and nitrogen blowdown. Mirex was added to PUF-PAS sample extracts as an internal standard before splitting them into two equal halves by volume. The first half of the sample was reconstituted in isooctane along with the addition of respective standards, and was used for the non-target analysis of OPFR transformation products. The other half of the sample was eluted through a silica column followed by addition of OPFR internal standards and re-constituting the final volume in methanol, which was used for the target-analysis of parent OPFRs (see Supplementary Information). The oxidation flow reactor samples were not split into two halves and the entire volume was reduced to 0.5 mL using acetonitrile as a solvent without addition of any standards.

Sampling volume. The equivalent sampling air volume (Veq, m^3) was estimated using the GAPS template.[34] This template takes into consideration the PUF-air partition coefficient for each target analyte and average temperature of the sampling period for correction of Veq, and has been used previously under the GAPS network and other regional studies.[2,13] A generic sampling rate of 4m^3 day^{-1} was used for calculations.[13]

Oxidation flow reactor (OFR) experiments

Experiments investigating the heterogeneous OH oxidation of 9 different types of OPFR particles were performed using an OFR.[35] Seed particles of $(NH_4)_2SO_4$ were generated via atomization (TSI, model 3706), dried through a diffusion drier (TSI, model 3062), and passed through the headspace of a temperature-controlled Pyrex tube (343 K) containing a pure OPFR, to produce coated particles with a calculated coating thickness of ~15 nm based upon the shift in the peak of the particle size distribution which was measured using a TSI scanning

mobility particle sizer. For TCEP and TCPP, pure organic particles were generated by sending an aqueous solution of each organic through a TSI atomizer and drawn through a diffusion drier. Those OPFR particles were introduced into the OFR and were exposed to O_3 (0–2 ppm) under 254 nm UV light irradiation at 298 K in each experiment. OH radicals were generated by the photolysis of O_3 at 254 nm followed by reaction with water vapor (35% RH). In offline calibrations, the OH exposure was calculated through the loss of CO due to its reaction with OH,[36] and was in the range of 1.2×10^{11}–1.6×10^{12} molecules cm^{-3} s. Further details regarding the OFR experiments are provided in the Supplementary Information.

The particulate OPFR products formed from heterogeneous OH reactions were measured using a recently developed extractive electrospray ionization time-of-flight mass spectrometer (EESI-TOFMS).[22,35] Briefly, the particle-containing flow exiting the flow tube reactor passed through a multichannel extruded carbon denuder at the inlet of the EESI-TOFMS which removed most of the gaseous species with high efficiency.[22] The oxidized OPFR particles then collide with electrospray droplets generated at the end of an electrospray capillary (New Objective; #TT360–50–50–N–5) at a flow rate of 1 μL min^{-1}. Soluble components of the particles were extracted, ionized through a Coulomb explosion of the charged droplets, and detected by a Tofwerk APi-TOFMS. The electrospray working solution was a water-acetonitrile mixture (1:1 by volume) with 110 ppm of sodium iodide as a charge carrier. The mass spectra were recorded in positive ion mode (i.e., Na^+ adducts).

Non-target analysis

GC-APCI-TOFMS measurement. Using an NTA method described previously,[37] the offline OFR sample extracts and ambient air extracts from the GAPS-MC network were analyzed using a gas chromatography (GC, Agilent 7890) system coupled with a quadrupole time-of-flight mass spectrometer (Waters Xevo G2XS). Sample extracts of 1 μL were injected into a desorption liner placed inside of a Gerstel thermal desorption and cooled injection system (model CIS-4) using a Gerstel multi-purpose autosampler. Upon injection, the temperature of the thermal desorption unit was rapidly ramped from 30 to 320 °C at 12 °C min^{-1} to evaporate analytes which were trapped on the CIS at 30 °C. The temperature of CIS was then ramped to 320 °C at 12 °C min^{-1} to load analytes to a DB-5HT column (J&W Scientific, 15 m length, 250 μm i.d, 0.10 μm film thickness). Chemicals loaded onto the column were separated using 3 mL min^{-1} of helium as the carrier gas. The GC temperature program ramped from 90 °C to 115, 150, 210, 280, 310 and 330 °C at rates of 95, 65, 45, 35, 30 and 25 °C min^{-1} respectively, followed by isothermal heating at 330 °C for 3.67 min. The temperature of the transfer line between the GC oven and the ionization source was set at 340 °C. An atmospheric pressure chemical ionization (APCI) source (positive ion mode, 150 °C, corona current: 3.0 μA, cone gas: 180 L h^{-1}) was employed to ionize chemicals eluted from the GC column. As a soft ionization technique, APCI preserves analyte molecules as $[M]^+$ or $[M+H]^+$ via charge exchange between N_2^+ and analyte molecules M or proton exchange between H_3O^+ and M.

Identification of transformation products. The NTA GC-APCI-TOFMS data were analyzed using MassLynx 4.2 (Waters Inc.). For offline OFR samples, the potential products were screened on the basis of a product list (Supplementary Table 1) obtained from online OFR measurements (step a in Fig. 1). In this step, we observed 27 products in offline OFR samples collected from 5 oxidized OPFRs (TCEP, TCPP, TDCPP, TBEP, and TPhP), with detailed information (retention time, m/z peak, isotopic patterns, chemical formula, and chemical structure) given in Supplementary Table 2. The number of detected transformation products in offline OFR samples and in ambient samples using this method were less than those detected in OFR online experiments (128 products for the 5 OPFRs mentioned above). This is expected, as some products may be below the method detection limits for the transformation products. Also, it is known that some oxidized products (e.g., peroxides) are likely to undergo decomposition during sample collection and extraction due to their high reactivity (i.e., having a short lifetime).[38] Finally, the number of transformation products identified in ambient samples here, are likely to represent only a fraction of the products which exist, due to the potential for decomposition of oxidized species at high temperatures[39] often associated with GC systems.

Unidentified OPFR products. In addition to the 11 identified OPFR products, we observed 9 unidentified products in the GAPS-MC field samples (Supplementary Table 3). Their chemical formulae are tentatively proposed according to their mass peaks and isotopic patterns (Supplementary Fig. 4). They are considered “unidentified products” for two reasons: (1) some of the products in Supplementary Table 3, which were included in our product list obtained from OFR experiments (Supplementary Table 1), had mass uncertainty greater than 20 ppm (e.g., U_2 and U_4 in Supplementary Table 3). (2) several products were not observed in the OFR experiments (i.e., not included in our product list), and their chemical structures are unknown. While the chemical structures of these products are unclear, we may infer their source (parent compounds) from the proposed chemical formulae. Given that all of these unidentified products exhibit clear ^{37}Cl isotopic patterns (Supplementary Fig. 4), they are originated from chlorinated OPFRs such as TCEP, TCPP, and TDCPP. The volume normalized signal intensities of 9 unidentified products in 18 megacities are shown in Supplementary Fig. 5. It is interesting to note that London, UK and New York, USA possess the highest overall signal intensities (36.6 counts m^{-3} for London and 5.1 counts m^{-3} for New York). This is consistent with the observed high levels of parent chlorinated OPFRs (>10000 pg m^{-3})[13] and high levels of identified chlorinated transformation

products in these two cities (Fig. 3a). The consistency of the levels of chlorinated OPFR parent compounds (TCEP, TCPP, and TDCPP), identified chlorinated products (e.g., TCEP-1, TCPP-21, and TDCPP-14) and the sum of the unidentified chlorinated products (U_1–U_9) provides additional confirmation of our product identification.

In-silico modelling

RAIDAR model. Overall persistence and bioaccumulation were modelled using the Risk Assessment, Identification, And Ranking (RAIDAR) model. RAIDAR is a steady-state multimedia fate and exposure model in support of high-throughput hazard and risk assessments for chemical substances.[40,41] RAIDAR has been successfully applied to screen and prioritize more than 10 thousand neutral and ionogenic organic chemicals within the markets of OECD (Organization for Economic Co-operation and Development) countries, the US, and Canada.[42-46]

RAIDAR is a mechanistic model (Supplementary Fig. 6), it builds upon mechanistic descriptions of a series of physical, chemical, biological, and physiological processes governing chemical fate and exposure, which reflect the state-of-the-art understanding of chemical fate and toxicokinetics. It describes the transport and transformation of chemicals in a regional environment (a total area of 10^{11} m^2) comprising four bulk compartments: air (with a volume of 1.0×10^{14} m^3; gaseous and particle phases), surface water (2.0×10^{11} m^3; water and suspended solid phases), soil (1.8×10^{10} m^3; gaseous, pore water, and solid phases), and sediment (5.0×10^{8} m^3; water and solid phases). Here, the surface water, soil, and sediment can be collectively referred to as surface media. Chemicals undergo advection, diffusion, and transformation within and between these compartments. Notably, ionogenic organic chemicals can dissociate in the water phase of surface media (soil has a pH of 6 whereas other surface compartments share a pH of 7). The modeled region has an average temperature of 10 °C and annual precipitation of 876 mm, which represents a typical humid continental climate in North America. RAIDAR assumes that the advective air flow in the modeled region possesses a residence time of 100 hours, and the advective water flow in the modeled region possesses a residence time of 10^5 hours. We use the above default values in our assessment. The RAIDAR model outputs estimates of mass (M_i) and concentrations (C_i) of chemicals in individual environmental compartments.

Persistence. The "overall persistence (P_{OV})" is defined as the average time that a chemical resides in the multiple environmental compartments.[47,48] In RAIDAR, P_{OV} is mathematically expressed as the ratio of the total amount of chemical in the modeled region to the total rate of loss from the modeled region given by:[41]

$$P_{OV} = \frac{M_{total}}{N_{R,total}} = \frac{\sum_i M_i}{\sum_i (M_i \cdot k_i)} \quad (1)$$

where i = air, surface water, soil, and sediment. Equation 1 indicates that P_{OV} is determined mainly by two factors: (1) rates of chemical losses in individual environmental compartments, including the rates of reaction with OH radicals (for the air compartment) and biodegradation (for surface media), and (2) multi-compartmental distribution, which is governed by the phase partition behavior of the chemical of interest. Since P_{OV} is a hypothetical, integrative measure of a chemical's overall persistence in the multimedia environment, it is not observable in real-world studies. The higher the P_{OV}, the longer a chemical is present in the environment, and its contamination, once it occurs, is less reversible. P_{OV} is an integrative measure because it allows for the interplay between the multimedia distribution and degradation in individual media; that is, we can expect a high overall persistence if the property of a chemical favors its stay in an environmental medium where it undergoes negligible degradation. An advantage of using P_{OV} in this work is that we do not need to measure the yields of transformation products, given that P_{OV} is an intensive property, which is independent of the actual mass formed or present in the environment.

Bioaccumulation. The RAIDAR model also describes absorption, biotransformation, and excretion of chemicals in living organisms in terrestrial and aquatic food webs. Specifically, it contains a fish bioaccumulation module, which evaluates the accumulation of chemicals in the fish tissue from water by quantifying toxicokinetic processes including gill respiration, dietary ingestion, metabolic transformation, fecal egestion, and growth dilution. In doing so, RAIDAR estimates chemical concentrations (C_B) in the fish tissue. Mechanistically, the net accumulation of a chemical in the fish tissue is the difference between chemical flows entering and leaving the fish body; as such, a chemical would have a limited bioaccumulation potential if it easily departs from the fish body, e.g., due to a high rate of gill mass exchange (for highly soluble chemicals) or metabolic transformation (for less persistent chemicals).

Here, we calculated a "bio-concentration factor" (BCF; in L kg^{-1}) as the ratio of wet weight-based concentration of chemical in fish tissue (C_B, $g_{chem}/kg_{wet\ weight}$) to the total concentration of chemical in the surface water compartment (C_W, g_{chem}/L_{water}), assuming an absence of

dietary intake of the chemical by the modeled fish (i.e., gill absorption is the sole source of chemical to fish):

$$BCF = \frac{C_B}{C_W} \quad (2)$$

This manner of calculation is consistent with the common practice in OPFR bioaccumulation experimental studies.[49-52] BCF is a measurable indicator in real-world studies. Supplementary Table 5 compares RAIDAR predictions for OPFRs with observed BCF values collected from the literature, which indicates satisfactory agreement for most OPFRs investigated here.

RAIDAR requires properties of chemicals as basic inputs for the computation, including: (1) partition coefficients (K_{OW}, K_{AW}, and K_{OA}) (referred to as "distribution ratios", D_{OW}, D_{AW}, and D_{OA}, for ionogenic organic compounds) between the air, water, and n-octanol phases, (2) dissociation constants (pKa), (3) rate constants of environmental reactions with OH radicals (for calculating degradation in the air) and biodegradation (for calculating degradation in surface media), and (4) rate constants of biotransformation in fish. In this work, we use a quantitative structure-activity relationship (QSAR) model called "OPEn-QSAR-App (OPERA)" to predict partition coefficients for neutral transformation products.[53] For ionogenic transformation products, the partition coefficients of the neutral fractions are predicted using OPERA, whereas the partition coefficients of charged fractions are calculated from those of the neutral fractions based on an empirical relationship described previously.[54] The distribution ratios, which combine partition coefficients of the neutral and charged fractions, are then calculated using the Henderson-Hasselbalch equation. Dissociation constants (pKa) and rate constants of environmental reactions (2 &3 above) are also predicted using OPERA.[53,55] Rate constants of biotransformation in fish are predicted using a QSAR model named Iterative Fragment Selection (IFS).[56] Of the total of 195 investigated OPFR-related species (9 parent OPFRs + 186 transformation products), 190, 134, 72, and 179 have partition coefficient predictions, pKa predictions, environmental reaction rate constants, and biotransformation rate constants, within the domains of applicability of the QSAR models. Chemicals falling in the domain of applicability are of the highest confidence; however, chemicals outside the domains of applicability are also used in this work due to the lack of other available QSAR models at this point.

Toxicity. Toxicity is quantified using an oral 50% lethal dose (LD_{50}) for rats, which is defined as the dose of chemical (normalized by bodyweight) that can cause 50% of rats in a population to die after oral ingestion. A lower LD50 corresponds to higher toxicity. In this work, the toxicities of the OPFR transformation products were estimated using the Toxicity Estimation Software Tool (TEST).[57] TEST is a QSAR model in support of the prediction of various toxicological endpoints from a chemical's structure. Specifically, TEST first calculates a series of chemical-specific molecular descriptors based on the entire or partial features of a molecule, selects appropriate molecular descriptors based on pre-defined statistical algorithms, and then uses mathematical combinations of these molecular descriptors to predict toxicological endpoints. TEST's prediction algorithm for oral rat LD50 is based on a training set of more than 7,400 chemical substances.[57] For each compound, TEST employs three methods, i.e., the hierarchical, FDA, and nearest neighbor methods, to predict the oral rat LD50 and uses their average as a consensus estimate for output. Earlier statistical external validation indicates that the consensus model explains 62.6% of total variation observed among chemicals in the training set, with a root mean square error (RMSE) of 0.54 log units. Oral rat LD50 has previously been experimentally determined by toxicological studies for select OPFRs. Supplementary Table 5 compares TEST predictions for OPFRs with observed oral rat LD50 used as the TEST training set, which indicates satisfactory agreement for most OPFRs investigated here.

Note that our analysis (OPFR product identification and NTA) does not distinguish between positional isomers, i.e., isomers sharing the same functional groups but with different positions (such as ortho-, meta-, and para-aromatic substitutions). However, Supplementary Fig. 7 indicates that PBT differs only marginally between positional isomers. As such, it is acceptable to ignore positional isomers of transformation products in such high-throughput screening efforts.

Declarations

Acknowledgments

This work was supported by the Chemicals Management Plan (CMP) of Environment and Climate Change Canada.

Author contributions

Q.L., J.L., and T.H. designed the research. A.S. and T.H. led the GAPS-MC program. A.S. performed the target analysis experiments for parent OPFRs. X.Z. and C. Hao performed the non-target analysis experiments for GAPS-MC samples. Q.L., X.Z., and W.L. analyzed the non-target

mass spectra data. Q.L. performed the OFR experiments. L.L. performed the PBT modelling. Q.L., L.L., J.L., X.Z., A.S., T.H., H.H., C. Hao, W.L., K.L., P.L., J.J.B.W., C. Huo, and S.-M.L. contributed to the scientific discussions. Q.L., L.L., J.L., A.S., and X.Z. wrote the manuscript.

Competing interests

The authors declare no competing interests.

Additional information

Supplementary Information is available for this paper.

Correspondence and requests for materials should be addressed to J.L. or T.H.

Reprints and permissions information is available at www.nature.com/reprints.

References

1 Johnson, A. C., Jin, X., Nakada, N. & Sumpter, J. P. Learning from the past and considering the future of chemicals in the environment. *Science* **367**, 384-387 (2020).

2 Rauert, C., Schuster, J. K., Eng, A. & Harner, T. Global atmospheric concentrations of brominated and chlorinated flame retardants and organophosphate esters. *Environ. Sci. Technol.* **52**, 2777-2789 (2018).

3 Kahn, L. G., Philippat, C., Nakayama, S. F., Slama, R. & Trasande, L. Endocrine-disrupting chemicals: implications for human health. *Lancet Diabetes Endocrinol.* **8**, 703-718 (2020).

4 Christensen, F. M. *et al.* European experience in chemicals management: integrating science into policy. *Environ. Sci. Technol.* **45**, 80-89 (2011).

5 United Nations *World Urbanization Prospects*. https://population.un.org/wup/Publications/Files/WUP2018-Report.pdf (UN, 2018).

6 United Nations *Stockholm Convention*. http://www.pops.int/ (UN, 2004).

7 Escher, B. I., Stapleton, H. M. & Schymanski, E. L. Tracking complex mixtures of chemicals in our changing environment. *Science* **367**, 388-392 (2020).

8 Wei, G. L. *et al.* Organophosphorus flame retardants and plasticizers: sources, occurrence, toxicity and human exposure. *Environ. Pollut.* **196**, 29-46 (2015).

9 Sauvé, S. & Desrosiers, M. A review of what is an emerging contaminant. *Chem. Cent. J.* **8**, 1-7 (2014).

10 United States *Toxic Substances Control Act.* https://www.epa.gov/tsca-inventory (US, 1976).

11 European Union *Registration Evaluation, Authorization and Restriction of Chemicals.* https://echa.europa.eu/regulations/reach/understanding-reach (EU, 2007).

12 Mill, T., Patel, J. M. & Tebes-Stevens, C. The environmental fate of synthetic organic chemicals. *Phys. Sci. Rev.* **4** (2018).

13 Saini, A. *et al.* GAPS-megacities: A new global platform for investigating persistent organic pollutants and chemicals of emerging concern in urban air. *Environ. Pollut.* **267**, 115416 (2020).

14 Zhao, S. *et al.* Evidence for major contributions of unintentionally produced PCBs in the air of China: implications for the national source inventory. *Environ. Sci. Technol.* **54**, 2163-2171 (2019).

15 Salamova, A., Ma, Y., Venier, M. & Hites, R. A. High levels of organophosphate flame retardants in the Great Lakes atmosphere. *Environ. Sci. Technol. Lett.* **1**, 8-14 (2013).

16 Washington, J. W. *et al.* Nontargeted mass-spectral detection of chloroperfluoropolyether carboxylates in New Jersey soils. *Science* **368**, 1103-1107 (2020).

17 Hollender, J., Schymanski, E. L., Singer, H. P. & Ferguson, P. L. Nontarget screening with high resolution mass spectrometry in the environment: ready to go? *Environ. Sci. Technol.* **51**, 11505-11512 (2017).

18 Hites, R. A. & Jobst, K. J. Is nontargeted screening reproducible? *Environ. Sci. Technol.* **52**, 11975-11976 (2018).

19 Blum, A. *et al.* Organophosphate ester flame retardants: are they a regrettable substitution for polybrominated diphenyl ethers? *Environ. Sci. Technol. Lett.* **6**, 638-649 (2019).

20 Möller, A. *et al.* Organophosphorus flame retardants and plasticizers in airborne particles over the Northern Pacific and Indian Ocean toward the polar regions: evidence for global occurrence. *Environ. Sci. Technol.* **46**, 3127-3134 (2012).

21 Peng, Z. & Jimenez, J. L. Radical chemistry in oxidation flow reactors for atmospheric chemistry research. *Chem. Soc. Rev.* **49**, 2570-2616 (2020).

22 Lopez-Hilfiker, F. D. *et al.* An extractive electrospray ionization time-of-flight mass spectrometer (EESI-TOF) for online measurement of atmospheric aerosol particles. *Atmos. Meas. Tech.* **12**, 4867-4886 (2019).

23 World Health Organization *UNEP/IPCS training module No. 3 chemical risk assessment*. https://apps.who.int/iris/bitstream/handle/10665/66398/WHO_PCS_99.2_eng.pdf?sequence=1 (WHO, 1999).

24 Harrison, R. M. Urban atmospheric chemistry: a very special case for study. *NPJ Clim. Atmos. Sci.* **1**, 1-5 (2018).

25 Jimenez, J. L. *et al.* Evolution of organic aerosols in the atmosphere. *Science* **326**, 1525-1529 (2009).

26 Saini, A. *et al.* Flame retardants in urban air: a case study in Toronto targeting distinct source sectors. *Environ. Pollut.* **247**, 89-97 (2019).

27 Kelly, B. C., Ikonomou, M. G., Blair, J. D., Morin, A. E. & Gobas, F. A. Food web–specific biomagnification of persistent organic pollutants. *Science* **317**, 236-239 (2007).

28 Neumann, M. & Schliebner, I. *Protecting the sources of our drinking water: the criteria for identifying persistent, mobile and toxic (PMT) substances and very persistent and very mobile (vPvM) substances under EU Regulation REACH (EC) No 1907/2006*. (German Environment Agency, 2019).

29 Kalgutkar, A. S. *et al.* A comprehensive listing of bioactivation pathways of organic functional groups. *Curr. Drug Metab.* **6**, 161-225 (2005).

30 Zhang, Q., Yu, C., Fu, L., Gu, S. & Wang, C. New insights in the endocrine disrupting effects of three primary metabolites of organophosphate flame retardants. *Environ. Sci. Technol.* **54**, 4465-4474 (2020).

31 Vermeulen, R., Schymanski, E. L., Barabási, A.-L. & Miller, G. W. The exposome and health: where chemistry meets biology. *Science* **367**, 392-396 (2020).

32 Hystad, P. *et al.* Associations of outdoor fine particulate air pollution and cardiovascular disease in 157 436 individuals from 21 high-income, middle-income, and low-income countries (PURE): a prospective cohort study. *Lancet Planet. Health* **4**, 235-245 (2020).

33 United Nations *World Economic Situation and Prospects 2020*. https://www.un.org/development/desa/dpad/publication/world-economic-situation-and-prospects-2020/ (UN 2020).

Methods references

34 Harner, T. *Template for calculating PUF and SIP disk sample air volumes* https://www.researchgate.net/publication/340470431_2020_v2_Template_for_calculating_PUF_and_SIP_disk_sample_air_volumes_April_06 (2020).

35 Liu, Q. *et al.* Experimental study of OH-initiated heterogeneous oxidation of organophosphate flame retardants: kinetics, mechanism, and toxicity. *Environ. Sci. Technol.* **53**, 14398-14408 (2019).

36 Liu, Y. & Sander, S. P. Rate constant for the OH + CO reaction at low temperatures. *J. Phys. Chem. A* **119**, 10060-10066 (2015).

37 Zhang, X., Saini, A., Hao, C. & Harner, T. Passive air sampling and nontargeted analysis for screening POP-like chemicals in the atmosphere: opportunities and challenges. *Trends Anal. Chem.*, 116052 (2020).

38 Krapf, M. *et al.* Labile peroxides in secondary organic aerosol. *Chem* **1**, 603-616 (2016).

39 Buchholz, A. *et al.* Deconvolution of FIGAERO–CIMS thermal desorption profiles using positive matrix factorisation to identify chemical and physical processes during particle evaporation. *Atmos. Chem. Phys.* **20**, 7693-7716 (2020).

40 Arnot, J. A., MacKay, D., Webster, E. & Southwood, J. M. Screening level risk assessment model for chemical fate and effects in the environment. *Environ. Sci. Technol.* **40**, 2316-2323 (2006).

41 Arnot, J. A. & Mackay, D. Policies for chemical hazard and risk priority setting: can persistence, bioaccumulation, toxicity, and quantity information be combined? *Environ. Sci. Technol.* **42**, 4648-4654 (2008).

42 Arnot, J. A., Brown, T. N., Wania, F., Breivik, K. & McLachlan, M. S. Prioritizing chemicals and data requirements for screening-level exposure and risk assessment. *Environ. Health Perspect.* **120**, 1565-1570 (2012).

43 Ring, C. L. *et al.* Consensus modeling of median chemical intake for the US population based on predictions of exposure pathways. *Environ. Sci. Technol.* **53**, 719-732 (2018).

44 Arnot, J. A., Toose, L. & Armitage, J. *Generation of physical-chemical property data and the application of models for estimating fate and transport and exposure and risk potential for organic substances on the Canadian DSL* (Technical report for Environment and Climate Change Canada, 2018).

45 Arnot, J. A. & Armitage, J. M. *Parameterization and application of the RAIDAR model to aid in the prioritization and assessment of chemical substances.* (Technical report for Health Canada, 2013).

46 Arnot, J. A. & Mackay, D. *Risk prioritization for a subset of domestic substances list chemicals using the RAIDAR model (CEMC Report No. 200703)* (Technical Report for Environment and Climate Change Canada, 2007).

47 Klasmeier *et al.* Application of multimedia models for screening assessment of long-range transport potential and overall persistence. *Environ. Sci. Technol.* **40**, 53-60 (2006).

48 Webster *et al.* Evaluating environmental persistence. *Environ. Toxicol. Chem.* **17**, 2148-2158 (1998).

49 Tang, B. *et al.* Bioconcentration and biotransformation of organophosphorus flame retardants (PFRs) in common carp (Cyprinus carpio). *Environ. Int.* **126**, 512-522 (2019).

50 Bekele, T. G., Zhao, H., Wang, Y., Jiang, J. & Tan, F. Measurement and prediction of bioconcentration factors of organophosphate flame retardants in common carp (Cyprinus carpio). *Ecotox. Environ. Safe.* **166**, 270-276 (2018).

51 Wang, G. *et al.* Bioaccumulation mechanism of organophosphate esters in adult zebrafish (Danio rerio). *Environ. Pollut.* **229**, 177-187 (2017).

52 Muir, D., Yarechewski, A. & Grift, N. Environmental dynamics of phosphate esters. III. Comparison of the bioconcentration of four triaryl phosphates by fish. *Chemosphere* **12**, 155-166 (1983).

53 Mansouri, K., Grulke, C. M., Judson, R. S. & Williams, A. J. OPERA models for predicting physicochemical properties and environmental fate endpoints. *J. Cheminformatics* **10**, 10 (2018).

54 Trapp, S. & Horobin, R. W. A predictive model for the selective accumulation of chemicals in tumor cells. *Eur. Biophys. J.* **34**, 959-966 (2005).

55 Mansouri, K. *et al.* Open-source QSAR models for pKa prediction using multiple machine learning approaches. *J. Cheminformatics* **11**, 60 (2019).

56 Brown, T. N., Arnot, J. A. & Wania, F. Iterative fragment selection: a group contribution approach to predicting fish biotransformation half-lives. *Environ. Sci. Technol.* **46**, 8253-8260 (2012).

57 Martin, T. User's Guide for T.E.S.T. (version 4.2) Toxicity Estimation Software Tool: A Program to Estimate Toxicity from Molecular Structure. (Sustainable Technology Division, National Risk Management Research Laboratory, U.S. Environmental Protection Agency, Cincinnati, OH, (2016).

58 IQAir *2018 World air quality report* https://www.iqair.com/ca/world-most-polluted-cities (2018).

59 Croitoru, L., Chang, J. C. & Kelly A. *The cost of air pollution in Lagos*. http://documents1.worldbank.org/curated/en/980031575616020127/pdf/The-Cost-of-Air-Pollution-in-Lagos.pdf (The World Bank, 2020)

60 Sullivan, J. Trash or treasure: global trade and the accumulation of e-waste in Lagos, Nigeria. *Africa Today* **61**, 89-112 (2014).

61 Gravel, S. *et al.* Halogenated flame retardants and organophosphate esters in the air of electronic waste recycling facilities: evidence of high concentrations and multiple exposures. *Environ. Int.* **128**, 244-253 (2019).

Figures

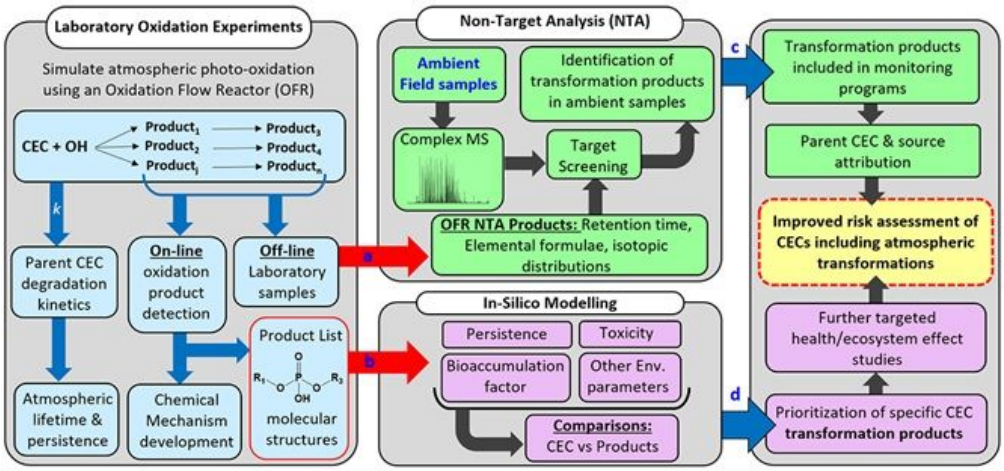

Figure 1

Framework developed for the improved risk assessment of CECs including atmospheric transformations. Laboratory oxidation experiments are used in this framework to derive reaction kinetics, develop transformation mechanisms and define the molecular structures and non-target analysis parameters of CECs transformation products. These are used as inputs to NTA of field samples (step a) and for in-silico property modelling (step b). Combined, the results of the framework can be used in the prioritization of CEC transformation products for further monitoring (step c) and targeted toxicity analysis (step d), leading to improved overall risk assessment of CECs which includes transformations in air. This framework is applied to organophosphate flame retardants in the current work, but is transferable to any CEC.

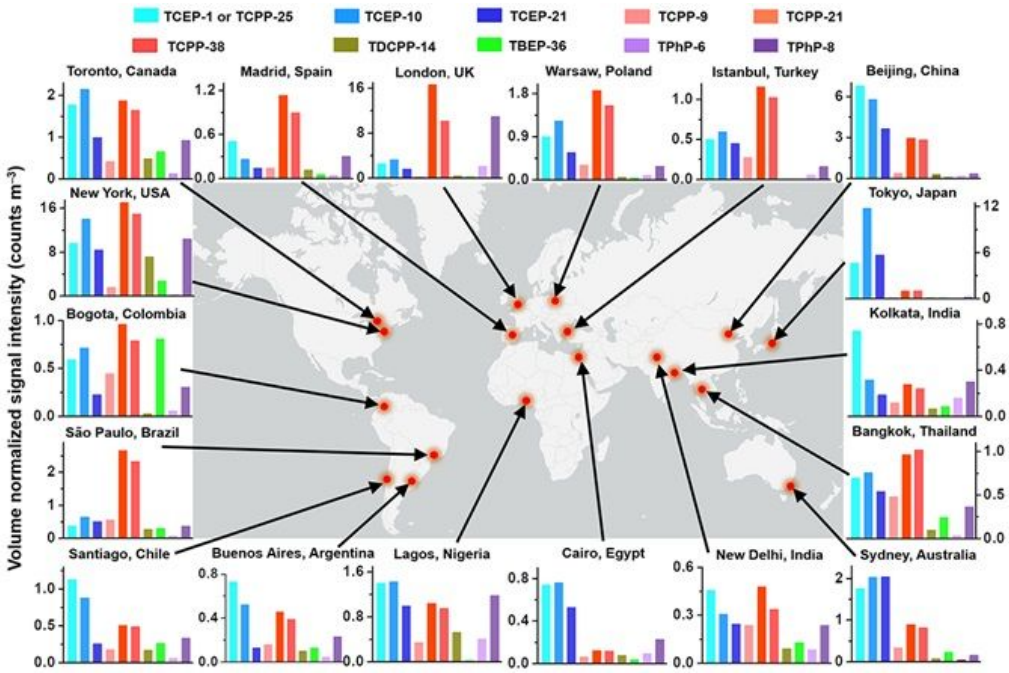

Figure 2

Global distribution of atmospheric OPFR transformation products. Volume normalized signal intensities (counts m–3) as proxies for concentrations of 11 OPFR transformation products in 18 megacities air samples collected in 2018–2019. Product TCEP-1 and TCPP-25 have the same chemical formula and are difficult to distinguish from each other (Supplementary Information). Sampling details are provided in Methods. The chemical structures of 11 identified OPFR products are shown in Extended Data Fig. 1. The results demonstrate that OPFR transformation products can be observed around the world, likely representing a lower limit to the true number of transformation products which exist. Note: The designations employed and the presentation of the material on this map do not imply the expression of any opinion whatsoever on the part of Research Square concerning the legal status of any country, territory, city or area or of its authorities, or concerning the delimitation of its frontiers or boundaries. This map has been provided by the authors.

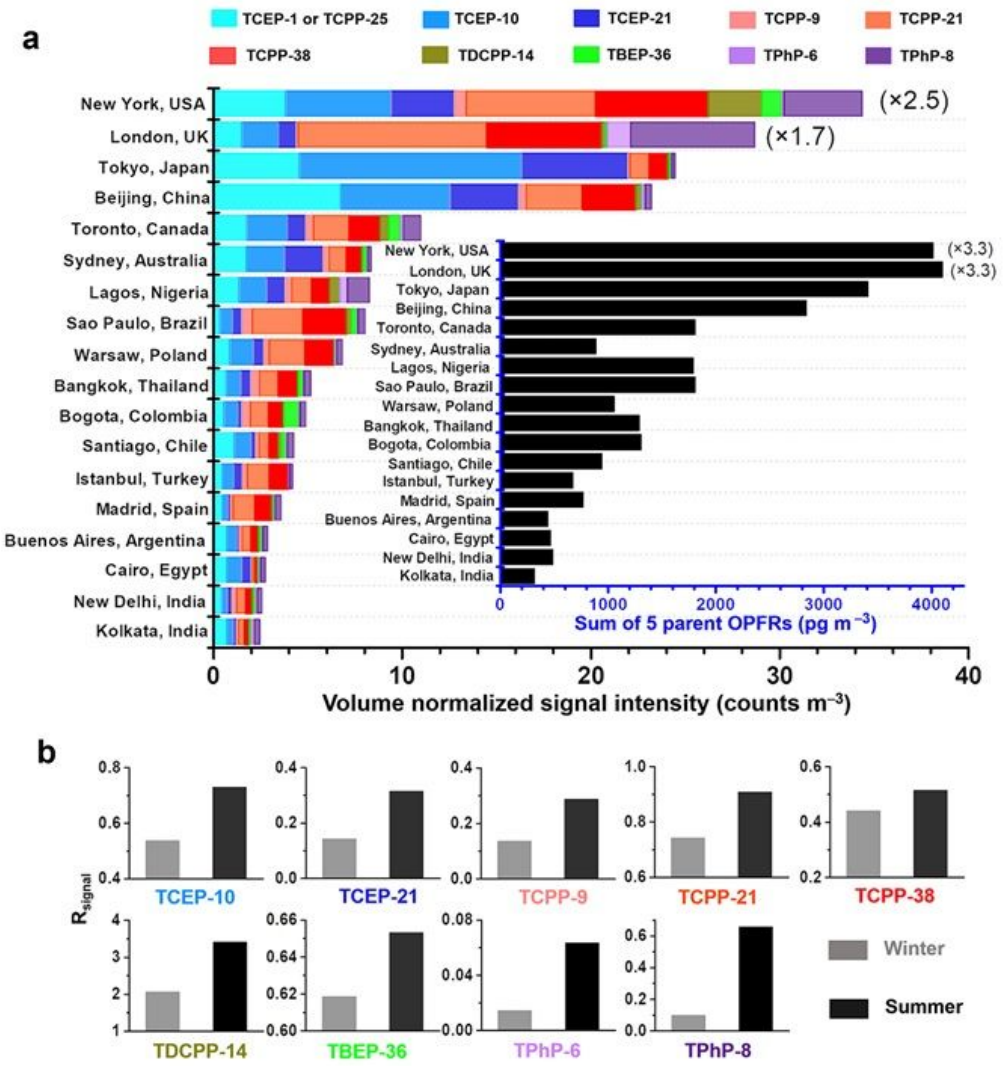

Figure 3

Sum of OPFR transformation products signal intensity in 18 megacities and their seasonal variations. a, Comparison between the sum of OPFR products and the sum of OPFRs from which they originated (inset) for the 18 megacities air samples collected in 2018–2019. For New York, and London, the signal intensities of parent OPFRs and their products equal the values shown in the figure × scaling factors. b, Seasonal variation of Rsignal in Toronto, Canada as a measure of photochemical production of OPFR products. Rsignal = the signal intensity of an OPFR product/the signal intensity of the corresponding parent OPFR. A higher Rsignal is indicative of increased photooxidation in the summer months. Samples were collected during summer (August–September, 2016) and winter (December 2016–January 2017)

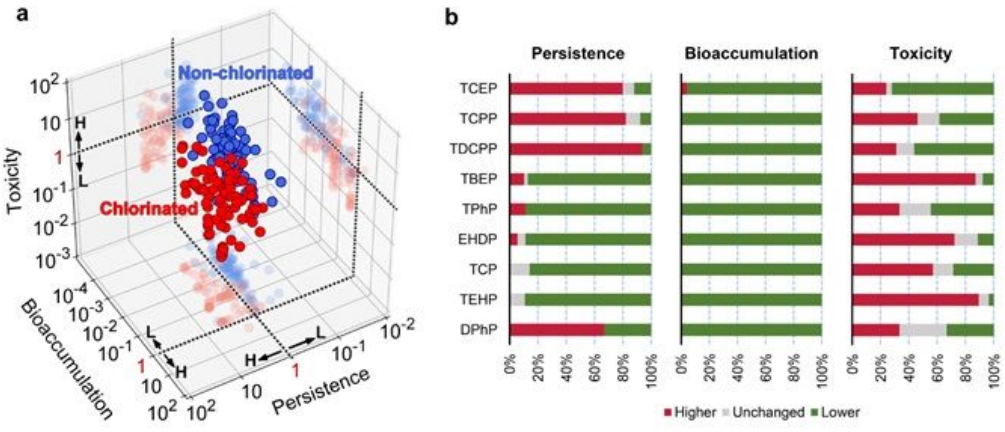

Figure 4

Persistence, bioaccumulation, and toxicity of OPFR transformation products relative to their parent compounds. a, Fold changes (in logarithm) in persistence, bioaccumulation, and toxicity of 186 transformation products relative to the 9 parent OPFRs from which they are derived. Transformation products of chlorinated and non-chlorinated OPFRs are shown as red and blue data points respectively. Dashed lines indicate no changes between product and parent molecule; arrows indicate the directions where the value of a given property becomes higher (H) and lower (L) than the parent molecule as a result of atmospheric transformation. For each parent-product pair, the fold change in persistence is calculated as the ratio between the product's and parent's overall persistence (in days) in the multimedia environment; the fold change in bioaccumulation is calculated as the ratio between the product's and parent's bioconcentration factors (in L/kg); the fold change in toxicity is calculated as the ratio between the parent's and product's oral rat LD50 (in mg/kg/d). b, Percentage of transformation products with a persistence, bioaccumulation capability and toxicity greater (red), less (green), and unchanged (grey) relative to the corresponding parent compounds. Properties within ±10% of the parent compound are considered unchanged.

Supplementary Files

This is a list of supplementary files associated with this preprint. Click to download.

- SupplementaryInformationV12.docx
- ExtendedData.pdf